Manipulation of low-energy spin precession in a magnetic thin film by tuning its molecular field

Valentin Desbuis, Daniel Lacour, Coriolan Tiusan, Christopher Vautrin, Sylvie Migot, J. Ghanbaja, Yuan Lu, Wolfgang Weber, Michel Hehn

Manipulation of low-energy spin precession in a magnetic thin film by tuning its molecular field

Valentin Desbuis,[1] Daniel Lacour,[1] Coriolan Tiusan,[2] Christopher Vautrin,[1] S. Migot,[1] J. Ghanbaja,[1] Yuan Lu,[1] Wolfgang Weber,[3] and Michel Hehn[1,*]

[1]*Institut Jean Lamour, CNRS – Université de Lorraine, 54011 Nancy, France*

[2]*Department of Solid State Physics and Advanced Technologies, Faculty of Physics, Babes-Bolyai University, Cluj Napoca 400114, Romania*

[3]*Institut de Physique et Chimie des Matériaux de Strasbourg, UMR 7504 CNRS, Université de Strasbourg, 23 Rue du Loess, BP 43, 67034 Strasbourg Cedex 2, France*

(Received 1 August 2023; accepted 11 December 2023; published 3 January 2024)

The low-energy electronic spin precession is measured in the molecular field of a CoAl thin film. Designed to have a low Curie temperature, the variation of the CoAl molecular field results in an electronic spin precession angle that varies with temperature. The behavior is observed for injection energies between 0.9 and 1.2 eV and the results are explained on the basis of an exchange field varying with temperature.

DOI: 10.1103/PhysRevB.109.024403

I. INTRODUCTION

When a beam of electrons with an initial spin-polarization vector $\boldsymbol{P}_0$ is injected into a ferromagnetic layer with magnetization $\mathbf{M_{AL}}$, the polarization vector $\boldsymbol{P}$ will exhibit a precessional motion around $\mathbf{M_{AL}}$. This precessional motion is described by two angles: the filtering angle, θ, that describes the reorientation of $\boldsymbol{P}$ towards $\mathbf{M_{AL}}$ and the precession angle, ε, that describes the precession of $\boldsymbol{P}$ around $\mathbf{M_{AL}}$ [Fig. 1(a)]. Oberli *et al.* [1] showed that precession angles of several tens of degrees per nanometer could be measured at high energies using free-electron experiments. This results from the huge molecular field of a ferromagnetic layer that is estimated to be of the order of several hundred to a thousand Tesla. For electron energies below the vacuum level (4–5 eV for ferromagnetic metals, such as Co and Fe), the energies of interest in spintronics applications, the electronic spin behavior in its out-of-equilibrium state is not well known even if used as a source of spin-transfer torque [2]. This lack of knowledge relays the impossibility of external beam source experiments giving access to energies below the vacuum level. Recent lab-on-chip experiments conducted on all solid-state devices gave first answers [3]. A net precession angle could be experimentally measured as a result of a huge precession angle of 700 deg/nm evaluated from the *k*-resolved band-structure calculation and the smearing of it due to the prcession layer roughness. The fine analysis of this precession requires the continuous variation of the spin precession angle by varying one parameter that is difficult to obtain in a unique sample.

In this study, we aim at measuring a continuous variation of the spin precession angle by modulating the molecular field of a ferromagnetic layer. Having an active magnetic precession layer composed of a material with Curie temperature less than room temperature, the molecular field would be strongly modulated, resulting in an effective electronic spin precession angle that evolves with temperature. In the simple picture of the Weiss theory, the molecular field is proportional to the magnetization of the sample. Since our Schottky diode is effective for a temperature range between 50 and 150 K, i.e., does not show either charge trapping or leakage current [3,4], we have used a magnetic material for which the magnetization varies strongly in this temperature range (50–150 K). We focus our attention on an alloy between a metal and a ferromagnetic material. We have chosen Al as the metal. Indeed, transition-metal aluminides (CoAl, NiAl, FeAl) are known to have a paramagnetic-ferromagnetic transition for compositions close to 50% of Al at room temperature [5].

II. ALL-SOLID-STATE DEVICE

The all solid-state device is based on a magnetic tunnel transistor (MTT) architecture [Fig. 1(b)] [4]. A spin-polarised current is extracted from the polarising layer and injected through a MgO tunnel barrier into the precession layer. With a magnetization direction $\mathbf{M_{AL}}$ perpendicular to $\boldsymbol{P}_0$, the spin polarisation of the electron precesses around it during the electron propagation. The injection energy in the precession layer is controlled by the bias voltage applied to the tunnel barrier allowing a spectroscopic analysis of the precession angle. This angle is analyzed through the giant magneto resistance effect occurring in the active layer/Cu/analyser spin valve [blue/orange/green rectangles in Fig. 1(b)]. By using both a tunnel barrier and a Schottky diode [Fig. 1(b)], we ensure that the collected electrons in the semiconductor always have an energy higher than 0.7 eV (height of the Schottky barrier) and that collected electrons cross the Cu/Si with in an acceptance angle of roughly 4.5° (at an energy of 1 eV). As a result, the collected electrons in Si moved ballistically across the spin valve with a trajectory perpendicular to the multilayer interfaces (see Ref. [3] for further details).

The stack we have used for this study is as follows: Pt(5)/IrMn(7.5)/Co(2)/Ta(0.5)/CoFeB(2)/MgO(2.5)/$Co_{50}Al_{50}$(5)/Cu(3.5)/$[Ni(0.6)/Co(0.2)]_{x5}$/Ni(0.6)/Cu(5)/Ta(1)/Cu(5)//Si [100], where numbers in brackets indicate the layers thicknesses in nanometers. The multilayer is grown by sputtering on a hydrofluoric acid cleaned Si substrate [3,4]. The CoFeB layer is the polariser and $Co_{50}Al_{50}$ is the

*michel.hehn@univ-lorraine.fr

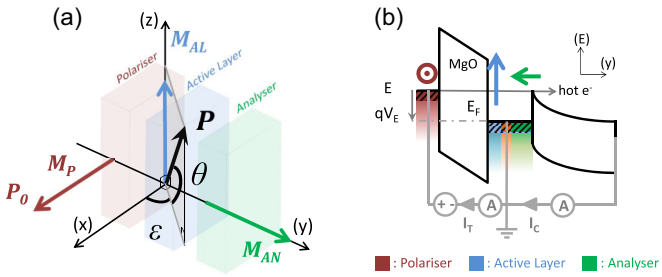

FIG. 1. (a) Precession and filtering angles for a beam of spin-polarized electrons $\mathbf{P_0}$ injected into a magnetic layer with magnetization $\mathbf{M_{AL}}$. The polarization after crossing the layer with $\mathbf{M_{AL}}$ is analyzed by the layer with . (b) Energy landscape experienced by the electrons. The dotted red circle represents the arrow of the magnetization of the polarizer layer pointing perpendicular to the paper sheet. The blue arrow represents the magnetization of the active layer and the green arrow represents the magnetization of the analyzer layer. See text for further details.

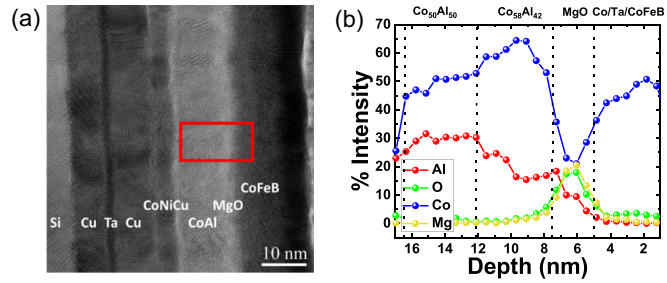

FIG. 2. (a) High-resolution transmission electron microscopy (HRTEM) micrograph of studied sample. (b) Chemical analysis by energy-dispersive x-ray analysis of the CoAl(10)/MgO/CoFeB interface made in the red rectangle. See text for further details.

active precession layer. The [Ni(0.6)/Co(0.2)]x5/Ni(0.6) multilayer represents the analyser and has its magnetization perpendicular to the film plane. The optimization of the three-dimensional magnetic configuration needed for the precession experiment has been done in Ref. [3]. Here, the Co or CoFeB precession layer used in Ref. [3] has been replaced by $Co_{50}Al_{50}$ (see the text below). Since this precession layer has an in-plane magnetization, no difficulty has been encountered to stabilize the three dimensional configuration of Fig. 1. This all solid-state platform for precession studies at low energies has been optimized in previous studies and details on the optimization of the magnetic properties or magnetocurrent contrast can be found in Refs. [3,6].

III. PROPERTIES OF Co_xAl_{1-x} LAYERS AND Co_xAl_{1-x} BASED MAGNETIC TUNNEL JUNCTION

In order to calibrate the magnetic response versus composition for our use in thin films, the magnetization has been measured in Si/Ta(5)/Pt(5)/Co_xAl_{1-x}(40)/Pt(5) as a function of x (see Ref. [4]). A 40-nm-thick Co_xAl_{1-x} was used to get a significant magnetic signal. We confirmed that for x less than 0.6, the alloy is not magnetic at room temperature. The magnetization versus temperature for x between 0.4 and 0.6 has been measured and we select the $Co_{50}Al_{50}$ alloy for our experiments [4].

The crystallographic and chemical properties of the $Co_{50}Al_{50}$ alloy were checked in the MTT multilayer stack by cross-sectional transmission electron microscopy (TEM). Figure 2(a) shows a high-resolution bright-field micrograph of the studied sample. As expected from previous work [6], the Cu(3.5)/[Ni(0.6)/Co(0.2)]$_{\times 5}$/Ni(0.6)/Cu(5) multilayer deposited on top of Ta(1)/Cu(5)//Si[100] exhibits as well-defined (111) texture that promotes a magnetization perpendicular to the film in the [Ni/Co] multilayer. The growth of the CoAl alloy does not follow this texture and shows grains with a chemically disordered body-centered cubic structure without a particular texture. This will have an impact on the model that will be used to analyse the precession results. A closer look at Fig. 2(b) (a chemical profile through the CoAl layer performed by energy-dispersive x-ray analysis) gives further details on the chemical composition of the CoAl alloy. This measurement has been performed on a 10-nm-thick CoAl sample. The CoAl layer extends from 7.5 to 17-nm depth and a clear diffusion of Al into MgO can be observed. Far from the MgO interface, for depths between 12 and 16 nm, Co and Al contribute, respectively, 50 and 30% to the measured signal. Considering this part to be preserved from any diffusion process, this intensity ratio is assumed to correspond to $Co_{50}Al_{50}$, the nominal composition of the alloy. Close to the MgO interface, the intensity ratio varies between 57/17 and 64/16 that corresponds to an atomic concentration between $Co_{64}Al_{36}$ and $Co_{52}Al_{48}$. We will consider the 5 nm of CoAl in contact with MgO homogeneous with an average concentration of $Co_{58}Al_{42}$. The fact that Al is pumped towards MgO can be understood considering the formation Gibbs energies which, in normal conditions, give the possible chemical reactions and underline those which are thermodynamically possible. At the CoAl/MgO interface, it is thermodynamically favorable to pump Al from $Co_{50}Al_{50}$ and form Al_2O_3 ($\Delta_f G* = -1582.3$kJ/mol) that is far more stable than MgO ($\Delta_f G* = -569.3$kJ/mol). Consequently, at the interface, this segregation phenomenon will lead to the formation of a Co-rich CoAl alloy.

Since no results have been reported in literature for such kind of magnetic tunnel junction (MTJ), the tunnel magnetoresistance (TMR) has been characterized. Figure 3 shows the tunnel magnetoresistance measured for different temperatures between 20 and 180 K for an applied voltage of 10 mV. The limited TMR value is ascribed to the polycrystalline CoAl structure that does not allow symmetry filtering as observed in CoFeB-based MTJs. Therefore, minority spin electrons probably contribute to the tunnel current, reducing the overall TMR of our device. The TMR decreases when temperature increases and seems to vanish for a temperature estimated to be around 225 K. This value is between the Curie temperatures measured for $Co_{55}Al_{45}$ and $Co_{60}Al_{40}$ and corresponds to an intermediate value of CoAl concentration as expected from the TEM analysis. In the following, the hot electron current and precession angle have only been measured for temperature less than 120 K where TMR is the highest and leakage current in the Schottky barrier is the lowest [4].

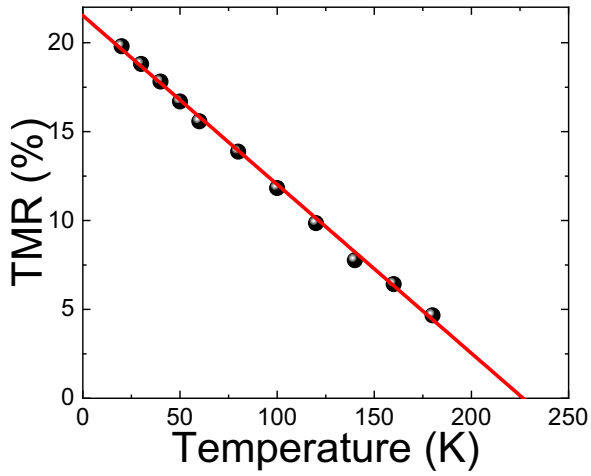

FIG. 3. TMR of the $Co_{50}Al_{50}$(5)MgO(2.8)CoFeB(2)Ta(0.5)Co(2) IrMn(7.5) tunnel junction as a function of the temperature measured at 10 mV.

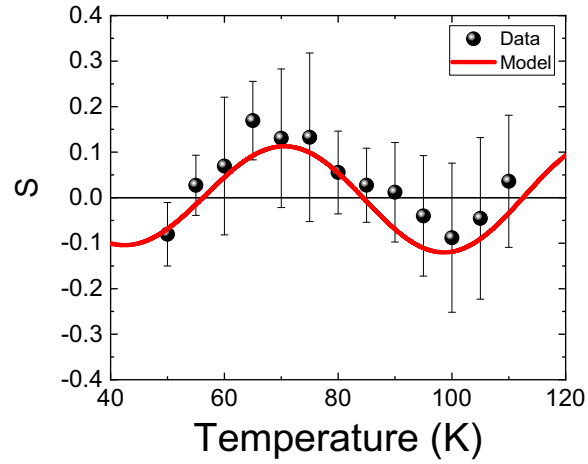

FIG. 4. S vs temperature for $V_E = -1.0$ V (dots) and fit using the model of spin precession (red line). Fit parameter: $\varepsilon^* = 289°/\text{nm}$, $\lambda^- = 0.93$ nm, and interface dephasing equal to zero.

IV. SPIN PRECESSION IN Co_xAl_{1-x}

The transfer ratio of the MTT, T_R, defined as the collected hot electron current I_C divided by the injected current through the tunnel barrier I_T, has been shown [3] to be equal to

$$T_R = T_R^{\perp}[1 + MC^{\perp}\, P_0 \cos(\theta)\sin(\varepsilon)], \tag{1}$$

where $MC^{\perp}$ is the magnetocurrent ratio defined as $\frac{I_C^{\parallel} - I_C^{\perp}}{I_C^{\perp}}$, where $I_C^{\parallel}$ and $I_C^{\perp}$ are the collected currents when **P** and $\mathbf{M}_{An}$ are parallel or perpendicular to each other, respectively. The $\cos(\theta)\sin(\varepsilon)$ product is obtained by measuring the transfer ratio in different configurations. The first one is the parallel configuration, $\parallel$, in which the active layer and analyzer are parallel such that $T_R^{\parallel} = T_R^{\perp}(1 + MC^{\perp}\, P_0)$. Then, T_R with precession in clockwise, $\circlearrowright$, and counterclockwise, $\circlearrowleft$, rotation can be measured by reversing the magnetization of the precession layer $\mathbf{M_{AL}}$ for a fixed direction of the analyzing layer $\mathbf{M_{AN}}$ (the magnetization of the [Co/Ni] multilayer). These two transfer ratios $T_R^{\circlearrowright}$ and $T_R^{\circlearrowleft}$ are expressed as $T_R^{\circlearrowright/\circlearrowleft} = T_R^{\perp}[1 \pm MC^{\perp} P_0 \cos(\theta)\sin(\varepsilon)]$. Finally, the direction of $\mathbf{M_{AN}}$ can also be reversed leading to two other $T_R^{\circlearrowright/\circlearrowleft}$ in which $\pm$ becomes $\mp$. As a result, the $\sin(\varepsilon)\cos(\theta)$ product as a function of experimentally available quantities is written as

$$S = \frac{T_R^{\circlearrowright} - T_R^{\circlearrowleft}}{2T_R^{\parallel} - (T_R^{\circlearrowright} + T_R^{\circlearrowleft})} = \sin(\varepsilon)\cos(\theta). \tag{2}$$

As shown in Ref. [4], inverting the direction of $\mathbf{M_{AN}}$ changes the sign of S and so of $\sin(\varepsilon)\cos(\theta)$ as expected from the previous discussion. Therefore, we have confidence in the results of our measurements. Figure 4 reports the measurement for $V_{\text{inj}} = -1$ V and temperature varying between 50 and 110 K: an oscillation of S can be observed. This strongly suggests a huge variation of the precession angle with temperature.

Considering electrons overcoming the Schottky barrier with $\vec{k}_{//} = \vec{0}$, no phase change while crossing interfaces, and the exponential decrease of the hot electron current with d (the thickness of the precession layer), we have shown in Ref. [3] that the S can be rewritten as

$$S = \sin(\varepsilon^* d)\cosh\left(\frac{d}{2\lambda^-}\right)^{-1}, \tag{3}$$

where ε^* is the precession angle per nanometer and $\frac{1}{\lambda^-} = \frac{1}{\lambda^{\downarrow}} - \frac{1}{\lambda^{\uparrow}}$ ($\lambda^{\downarrow\uparrow}$ being the minority/majority inelastic electron mean-free paths). Undoubtedly, the oscillation of the precession signal shown in Fig. 4 is a direct signature of a 360° change of $\varepsilon^* d$, such that ε^* varies over 70°/nm with a 55 K variation of temperature.

In real samples, however, fluctuations in the hot electron travel distance should be considered due to precession layer roughness. As a final step, a mean value of S was evaluated considering a travel distance varying from $d - \Delta d$ to $d + \Delta d$ for a sample with $d = 5$nm and a roughness of $\Delta d = 0.5$nm (obtained through TEM image analysis):

$$S = \frac{1}{\Delta d}\int_{d-\Delta d}^{d+\Delta d} \frac{\sin(\varepsilon^* . t)}{\cosh\left(\frac{t}{2\lambda^-}\right)} dt. \tag{4}$$

The expression of $\boldsymbol{\varepsilon^*}$, used in Ref. [3] and based on the k-vector resolved band structure, could not be used here due to the polycrystalline nature of CoAl. Therefore, we use the expression derived by Weber *et al.* [7]:

$$\boldsymbol{\varepsilon}^* = \sqrt{\frac{\boldsymbol{m_e}}{2\hbar^2}}\frac{\Delta \boldsymbol{E_{ex}}}{\sqrt{\boldsymbol{E}}}. \tag{5}$$

Considering a distance of segregation to the MgO interface [Fig. 2(a)] of about 5 nm, which is also the thickness of our CoAl used for the precession measurements, we assume that precession happens in an alloy with an atomic cobalt concentration about 58%. In the Weiss theory, the molecular field is proportional to the magnetization which depends on temperature. In the case of Ni, this has also been forecasted and experimentally verified [8]. We consider here that alloying the Co with Al will bring one additional electron to the Co atom, making its electronic configuration close to the one of Ni. This result needs to be more deeply studied in the future. Nevertheless, we modeled the variation of $\Delta \boldsymbol{E_{ex}}$ with

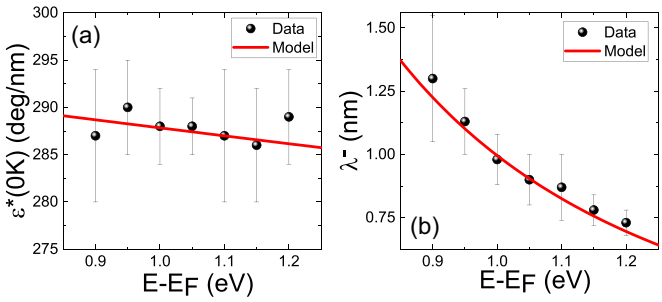

FIG. 5. Precession speed at 0 K (a) and spin length asymmetry (b) for the range of energy studied. Both parameters are extracted from fits using (5).

temperature using the linear variation of magnetization with temperature between the variations of $Co_{55}Al_{45}$ and $Co_{60}Al_{40}$ (see Supplemental Material [4]).

As a result, we rewrite (5) as

$$\boldsymbol{\varepsilon}^* = \sqrt{\frac{\boldsymbol{m_e}}{2\hbar^2}}\frac{\Delta \boldsymbol{E_{ex}}}{\sqrt{\boldsymbol{E}}} = \boldsymbol{\varepsilon}^*(\boldsymbol{E},0)\left(1-\frac{\boldsymbol{T}}{\boldsymbol{T_C}}\right), \tag{6}$$

with a Curie temperature of the alloy of 225 K [4].

The experimental values of S could be fitted (red solid line in Fig. 4) using (4) and (6). Error bars shown here are calculated from standard deviations for a dataset going from three up to ten precession measurements. The same procedure has been applied for energies between 0.9 and 1.2 eV [4], the highest energy being lower than twice the Schottky barrier height to avoid the contribution of secondary electrons. Extracted parameters from fits, namely precession speed at 0 K, $\boldsymbol{\varepsilon^*}(\boldsymbol{E},0)$, and the spin length asymmetry λ^-, are reported in Fig. 5 with associated error bars given by standard deviation of fitting parameters.

V. DISCUSSION

First, let us look at λ^- in Fig. 5(b). Spin length asymmetry is expressed as $\frac{1}{\lambda^-} = \frac{1}{\lambda^\downarrow} - \frac{1}{\lambda^\uparrow}$, ($\lambda^{\downarrow/\uparrow}$ being the minority/majority inelastic mean-free path). From our analysis and for the energy range of interest [−1.2 V;−0.9 V], λ^- lies between 0.7 and 1.5 nm, decreasing when energy increases. Reported values of λ^- in the literature using different Co-based alloys [3,9,10] are consistent with values found in this study. However, these values are higher than that reported for Co (1.4 nm) or CoFe (0.56 nm), which is expected considering Al has a much higher mean-free path than Co and that the magnetic moment of CoAl is much lower than the one of Co or CoFe. The energy dependence of λ^- could be reproduced assuming Coulombian inelastic interactions between hot electrons described using

$$\lambda^{\downarrow/\uparrow} = \lambda_0^{\downarrow/\uparrow}\frac{\sqrt{E}}{(E-E_F)^2}\,. \tag{6}$$

By leaving $\lambda_0^{\downarrow/\uparrow}$ as only free parameters, inelastic mean-free path for minority (majority) electrons is 0.95 nm (18.3 nm) for $E - E_F = 1$ eV [Fig. 5(b)]. Those values do not strongly depend on the other fitting parameter $\boldsymbol{\varepsilon^*}(\boldsymbol{E},0)$.

On the other hand, $\boldsymbol{\varepsilon^*}(\boldsymbol{E},0)$ is mostly constant with a value around 287 deg/nm. This value is more than two times lower than the one measured in CoFe, which was close to 700 deg/nm. As no phase change is considered at the MgO/CoAl interface, which is in accordance with theoretical predictions in magnetic multilayers [11], the energy dependence of $\boldsymbol{\varepsilon^*}(\boldsymbol{E},0)$ can be fitted using Weber's formula (5). The Fermi level is supposed to be that of the bulk Co (11.9 eV [12]). A slight variation of the inner potential by adding an electron from Al has little impact on the value of the exchange field fitted with this model. Based on (5), the model predicts a slow decrease of $\varepsilon^*(0\ \mathrm{K})$ with increasing energies which fits experimental data. Considering an effective electron mass equal to 1, the value for ΔE_{exch} obtained in this study is 6.92 eV, much higher than the exchange splitting in the Co band structure [13]. This high value of ΔE_{exch} needs to be explained and more deeply analyzed in future theoretical studies. However, TM_xAl_{100-x} alloys with x close to 50 are known to host a semiconducting-like resistivity versus temperature behavior [14]. This behavior has also been measured in our sample [4]. Band-structure calculations predict flat density of states in the energy range of our study [15,16]. As a result, it is not excluded that the effective mass of the electron is much higher than 1, making it that an overestimation of ΔE_{exch} using Eq. (5) is done if $m_e = 1$ is used.

VI. CONCLUSION

Here, we show that the precession angle per nanometer $\boldsymbol{\varepsilon^*}$ can be controlled between 217 deg/nm at 55 K to 143 deg/nm at 110 K. A further extension of measure temperature, a reduction of the CoAl thickness, or a change in the CoAl composition will lead to precession angle of 90 deg/nm that could be implemented in a nanometer-scale device. Further developments are also needed to increase the dependence of precession angle with energy such that it could be easy to tune by the voltage across a tunnel barrier.

ACKNOWLEDGMENTS

This work has been partially supported by ANR SpinPress (Grant No. ANR-09-BLAN-0076). Experiments were carried out on IJL Project TUBE-Davm equipment funded by FEDER (EU), French PIA project "Lorraine Université d'Excellence (Grant No. ANR-15-IDEX-04-LUE), Region Grand Est, Metropole Grand Nancy and ICEEL. C.T. acknowledges funding from Project No. "MODESKY" ID PN-III-P4-ID- PCE-2020–0230, Grant No. UEFISCDI: PCE 245/02.11.2021.

M.H. and D.L. conceived the project; C.V., V.D., M.H., and D.L. were in charge of the thin-film growth and optimization of magnetic properties; S.M. prepared the sample for TEM observation; J.G. and V.D. made the TEM observation and analysis; V.D. and C.V. patterned the samples; Y.L. designed the lithography masks and optimized the Cu/Si Schottky barrier; V.D. and D.L. conducted the electronic transport under applied field experiment; C.T., V.D., W.W., D.L., and M.H. analyzed the data; and D.L. and M.H. wrote the manuscript. All authors contributed to the discussion.

[1] D. Oberli, R. Burgermeister, S. Riesen, W. Weber, and H. C. Siegmann, Total scattering cross section and spin motion of low energy electrons passing through a ferromagnet, Phys. Rev. Lett. **81**, 4228 (1998).

[2] D. Ralph and M. Stiles, Spin transfer torques, J. Magn. Magn. Mater. **320**, 1190 (2008).

[3] C. Vautrin, D. Lacour, C. Tiusan, Y. Lu, F. Montaigne, M. Chshiev, W. Weber, and M. Hehn, Low-energy spin precession in the molecular field of a magnetic thin film, Ann. Phys. **533**, 2000470 (2021).

[4] See Supplemental Material at http://link.aps.org/supplemental/10.1103/PhysRevB.109.024403 for the properties of CoAl layers: magnetic properties; electrical resistance versus composition and temperature; and crystallographic analysis made by x rays and transmission electron microscopy; for the leakage current of the Schottky interface; for the impact of the analyzer layer polarity on the precession angle; and on the precession as a function of energy. In the Methods section, the multilayer stack is detailed and also the lithography steps to get the MTT device.

[5] S. R. Butler, J. E. Hanlon, and R. J. Wasilewski, Electric and magnetic properties of B2 structure compounds: NiAl, CoAl, J. Phys. Chem. Solids **30**, 1929 (1969).

[6] C. Vautrin, D. Lacour, G. Sala, Y. Lu, F. Montaigne, and M. Hehn, Thickness and angular dependence of the magnetocurrent of hot electrons in a magnetic tunnel transistor with crossed anisotropies, Phys. Rev. B **96**, 174426 (2017).

[7] W. Weber, D. Oberli, S. Riesen, and H. C. Siegmann, The electron analogue to the Faraday rotation, New J. Phys. **1**, 9 (1999).

[8] T. J. Kreutz, T. Greber, and J. Osterwalder, Temperature-dependent electronic structure of nickel metal, Phys. Rev. B **58**, 1300 (1998).

[9] W. Weber, S. Riesen, and H. C. Siegmann, Magnetization precession by hot spin injection, Science **291**, 1015 (2001).

[10] S. van Dijken, X. Jiang, and S. S. P. Parkin, Spin-dependent hot electron transport in $Ni_{81}Fe_{19}$ and $Co_{84}Fe_{16}$ films on GaAs(001), Phys. Rev. B **66**, 094417 (2002).

[11] C. Petitjean, D. Luc, and Xavier Waintal, Unified drift-diffusion theory for transverse spin currents in spin valves, domain walls, and other textured magnets, Phys. Rev. Lett. **109**, 117204 (2012).

[12] F. Batallan, I. Rosenman, and C. N. Sommers, Band structure and Fermi surface of hcp ferromagnetic cobalt, Phys. Rev. B **11**, 545 (1975).

[13] V. L. Moruzzi, J. F. Janak, and A. R. Williams, *Calculated Electronic Properties of Metals* (Pergamon, New York, 1978).

[14] J. Barzola-Quiquia, E. Osmic, and P. Häussler, The magnetic properties of amorphous Al_xFe_{100-x} alloys investigated by the atomic structure, magnetoresistance and anomalous Hall effect, J. Magn. Magn. Mater. **526**, 167624 (2021).

[15] V. Sundararajants, B. R. Sahut, D. G. Kanherel, P. V. Panatt, and G. P. Das, Cohesive, electronic and magnetic properties of the transition metal aluminides FeAl, CoAl and NiAl, J. Phys.: Condens. Matter **7**, 6019 (1995).

[16] D. Nguyen Manht, D. Mayout, A. Pasturelt, and F. Cyrot-Lackmannt, Electronic structure and hybridisation effects in transition-metal-polyvalent-metal alloys, J. Phys. F: Met. Phys. **15** 1911 (1985).